Valency of Ligand-Receptor Binding Ignored by Pair Potentials

William Morton,[*,†] Stefano Angioletti-Uberti,[†] and Robert Vácha[‡,¶]

†*Department of Materials, Imperial College, London U.K.*

‡*CEITEC – Central European Institute of Technology, Masaryk University, Brno, Czech Republic*

¶*Department of Condensed Matter Physics, Faculty of Science, Masaryk University, Brno, Czech Republic*

E-mail: wm816@ic.ac.uk

Abstract

The valency of ligand-receptor interactions has been ill-reported and uncontrolled in simulation based studies. It was found that a change in curvature of a nanoparticle, strength of ligand-receptor interactions, or receptor concentration could each drastically change the valency of the system. While the focus of this study was primarily on spherical nanoparticles, it is postulated that other structures with non-uniform curvatures might also exhibit similar behaviors. Previous literature may not necessarily be rendered invalid by the findings here, especially when parameters like lower receptor concentrations, smaller nanoparticles, adjusted ligand-receptor interaction strengths, or weaker bonding potentials were employed. However, to ensure methodological robustness and repeatability in nanoparticle studies, this work recommends eliminating the use of pairwise functions to model ligand-receptor due to demonstrated inconsistencies.

Introduction

Over the past three decades, the use of nanoparticles as drug carriers has gained considerable attention, with drug molecules either adsorbed to the surface or internalised in the particle[1,2]. The optimisation of nanoparticle uptake has been vital for achieving targeted cell delivery and multifunctionality, allowing nanoparticles also to be utilised for imaging and photothermal therapies[3,4]. Fundamental research has focused on the uptake of nanoparticles, based on their synthesised geometry before proteins are adsorbed to the surface, by focusing on receptor-mediated endocytosis[5]. The uptake of these nanoparticles is spontaneous — that is, the uptake is not dependent on the effects of cell signalling pathways, unlike, for example, micropinocytosis.

Receptor-mediated endocytosis occurs rapidly, posing a challenge in capturing these events at nanometer resolution[6]. The only available information is often that a nanoparticle has been internalised within a specific time frame. Small snapshots of the entry mechanisms, achieved using cryogenic electron microscopy, can possibly offer a glimpse into the nanoparticle - membrane interactions, but results are not always guaranteed[7]. Due to their higher reproducibility and improved control, lipid vesicles are occasionally employed as simplified yet representative models of the cell membrane[8]. However, it is essential to note that studies using lipid vesicles can only examine spontaneous uptake[9,10,11,12]. The benefit being that if uptake is observed within a lipid model, it implies that the nanoparticle can be endocytosed within a cellular system via ligand-receptor interactions[13]. Computer simulations have overcome these limitations by modelling lipid membrane systems, estimating the mechanisms and kinetics of nanoparticle uptake.[14]

Complexities in observing the wrapping of nanoparticles make computer simulations a valuable tool for investigating the impact of factors such as shape, size, and surface composition on the process[15,16,17,18]. A standard computational model for studying the dynamics of nanoparticle wrapping relies on ligand-receptor interactions to drive uptake while excluding other cellular effects to isolate the impact of size and shape. The term ligand-receptor in-

teractions is frequently encountered in computational studies of nanoparticle uptake, and it is essential to define its biological context. No specific ligand or receptor is typically considered; instead, the model encapsulates the general concept of a short-range bond formation that induces membrane curvature. These interactions are valence-limited, implying that no more than one ligand can interact with each receptor at any one time[19,20]. This limitation is primarily due to excluded volume effects, which prevent a second ligand from binding to the same receptor site.

However, it is worth noting that in most, if not all, literature on modelling nanoparticle interactions with lipid bilayers using molecular dynamics(MD), ligand-receptor interactions are described using a purely distance-dependent pairwise interaction, implying that this valence limitation condition is not explicitly enforced[15,18,21,16,5,22]. Additionally, popular MD engines such as LAMMPS and ESPResSO lack any mechanism to limit the number of interactions in a pair potential[23,24].

While a ligand with a valency above 1 is not inherently inaccurate, these systems are specific, and the valency should be highly controlled within the experiment. This paper focuses on delineating the non-physical effects that can arise in this context, as well as proposing a simulation strategy to rectify these effects.

Methods

Due to the substantial size of most nanoparticle structures, a coarse-grained system is necessary to investigate particle wrapping. Surface evolver methods are a popular alternative that often requires less computational power but at the expense of biological relevance[25]. For this reason, coarse-grained membranes have maintained their popularity over the years, and we will focus on the widely used Cooke-Deserno 3-bead membrane model[26]. In coarse-graining the lipid membrane, three individual beads that constitute the lipid are typically connected using a FENE potential, as depicted in Equation 1, and the angle between all three beads

in the lipids is maintained using the harmonic potential seen in Equation 2.

$$U_{FENE}(r) = -\frac{1}{2}K_1 r_0^2 \ln\left[1 - \left(\frac{r}{r_0}\right)^2\right] + 4\epsilon\left[\left(\frac{\sigma}{r}\right)^{12} - \left(\frac{\sigma}{r}\right)^6\right] + \epsilon \tag{1}$$

$$U_{harmonic} = K_2(\theta - \theta_0)^2 \tag{2}$$

The pairwise potentials between individual beads are described by the Weeks-Chandler Anderson (WCA) potential in Equation 3, and the cosine potential used for lipid tails are seen in Equation 4. Equation 3 describes the non-bonding component of the potential energy between individual beads of the lipid model, which in practice, is a short-range repulsion that determines the relative size of each bead. The nanoparticle's surface utilises the same repulsive interaction between the head and tail beads to ensure that lipids do not enter the nanoparticle volume.

$$U_{wca}(r) = \begin{cases} 4\epsilon\left[\left(\frac{\sigma}{r}\right)^{12} - \left(\frac{\sigma}{r}\right)^6 + \frac{1}{4}\right] & r \leq r_c \\ 0 & r > r_c, \end{cases} \tag{3}$$

Equation 4 facilitates the formation of a lipid bilayer by creating an attractive potential between lipid tails.

$$U_{tail}(r) = \begin{cases} -\epsilon & r < r_c, \\ \epsilon\cos^2\left(\frac{\pi(r-r_c)}{2w_c}\right) & r_c \leq r \leq r_c + w_c, \\ 0 & r > r_c + w_c \end{cases} \tag{4}$$

In Equations 1-4, r is the distance between two beads, ϵ is the Leonard-Jones unit for energy, and σ is the Leonard-Jones unit for distance. These two units are seen throughout Equations 1-4 as both units of measurement, ϵ being the potential well depth and σ being separation distance, as well as the fundamental units themselves. Therefore, you may en-

counter that ϵ in a given potential is a multiple of the fundamental unit, ϵ. The equilibrium bond length between two beads in Equation 1, r_0, is 1.5σ, and K_1 is the spring constant with a value of $30k_BT\epsilon$. The equilibrium angle in Equation 2, θ_0, is maintained at 180° from the current angle formed by the three beads, θ, using a spring constant, K_2, of $10k_BT\epsilon$. The critical length in Equation 3, r_c, maintains the shape of the lipid, with $r_c = 2^{1/6}b$, where $b_{head,head} = b_{head,tail} = 0.95\sigma$ and $b_{tail,tail} = \sigma$ are used to maintain a cylindrical lipid. Equation 4 w_c is an additional cutoff parameter that can be altered with the system's temperature to change membrane rigidity.

The simulated membrane used in this study comprises 10,452 lipids, 50% of which are receptors. The membrane dimension is 77 x 77 σ with a WCA cut-off of 1.5σ and a temperature of $1\epsilon/k_B$ maintained by a Langevin thermostat with a dampening parameter of1.0τ[27,28,29] . A larger bilayer is used for nanospheres exceeding 12σ in radius, which is 98 x 98 σ. We simulate a tensionless membrane, where the zero-tension condition is maintained using a Nose-Hoover barostat in the XY plane parallel to the membrane, with a pressure dampening term of 1000τ. All simulations are performed using the LAMMPS program, and each system was simulated five times for $10^4\tau$, with a time-step of 0.01τ .

Ligand-receptor interactions can be modelled using any inter-atomic interaction potential. A common practice is to use the pair-potential in Equation 4 that is scaled to be shorter by multiplying the WCA cut-off by 0.3 ($WCA_{LR} = 0.45$), and making the strength of the interaction ϵ_{LR}[15] . The scaling is intended to help mimic the size and separation of ligand-receptor pairs. Unless otherwise stated $\epsilon_{LR} = 20\epsilon$. Using Equation 4 is a convenient solution, reducing the number of pair-potentials one must introduce into the system. However, for most MD engines, Equation 4 is only available as a pair-potential, where valency can not be imposed. Using a tabulated version of the potential in Equation 4 as a bond style, we could easily introduce valency into the system, controlling the maximum number of bonds that can be formed for each ligand or receptor. Bond breaking is allowed within the simulation, but caution must be taken to ensure that the bond energy at rupture is larger than the possible

fluctuation in temperature. For this specific system, rupture is set to occur when a bond length exceeds 1.5σ, corresponding to a ligand-receptor binding energy of 1.25ϵ. Since the mean temperature is 1ϵ with a standard deviation of $4.4x10^{-3}\epsilon$, there is no concern about a bond length exceeding the dissociation cutoff.

Receptors are commonly made abundant (around 50%), which could mimic the over-expression of receptors on the cell surface, common in cancerous cells, which are ideal for targeted drug-delivery, but more importantly, decrease the simulation time by eliminating diffusion-limited interactions[30]. This somewhat arbitrary choice influences the nanoparticle wrapping time. In most studies, one does not look at its absolute value but rather at the ratio to that of a sphere to gauge the effect of particle size and shape. These comparisons also help to translate simulated results into experimental data. The comparison can be estimated using a comparative wrapping time, T_w, between a nanoparticle of interest and a nanosphere where the experimental wrapping time or cellular uptake rate is known.

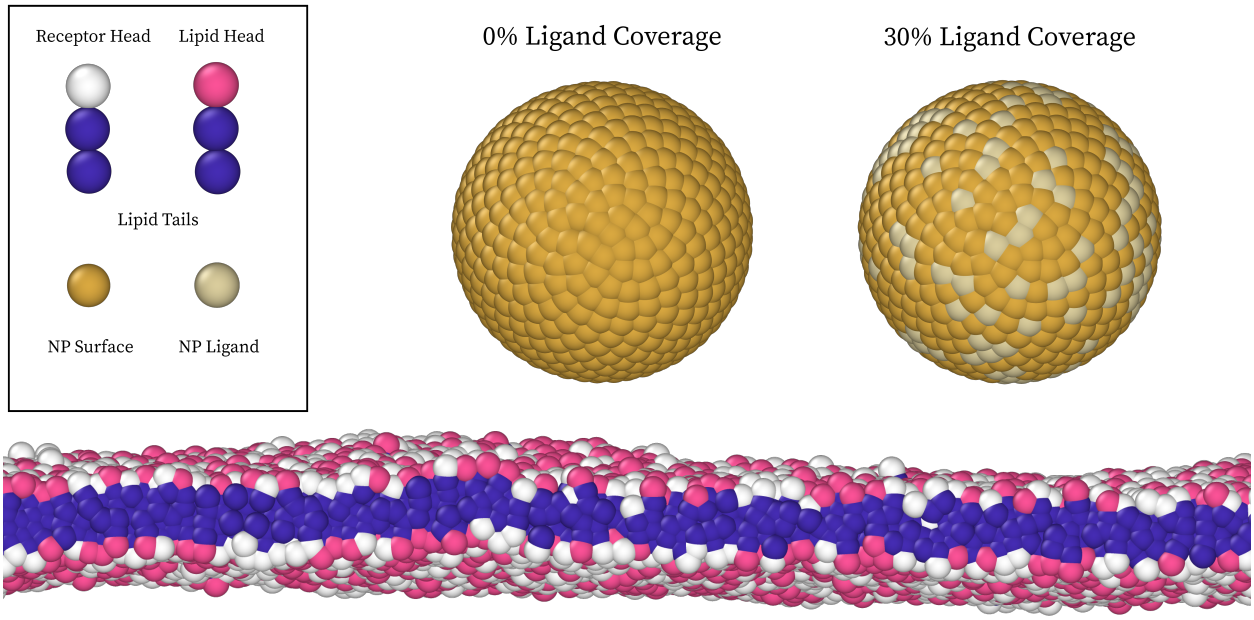

Figure 1: A visualisation of the lipid bilayer with two spherical nanoparticles with 0% (Left) and 30% (Right) of the surface area covered with ligands.

To provide a quantitative definition of valency when using simple distance-dependent in-

teractions, the time average ligand valency is calculated by $X = (\frac{1}{L}\sum_{n=1}^{L} U_{tail})/\epsilon_{LR}$ after the particle has been completely wrapped and equilibrated for $1e3\tau$. A long equilibration time ensures that the average valency is representative of the final state, where the nanoparticle is in a vesicle.

Results and Discussion

The impact of the nanosphere's geometric features, particularly the curvature, on ligand-receptor interactions is expected to be the main driving effect for the artificially increased valency exemplified in Table 1. In the context of a nanosphere, surface curvature is inversely proportional to the radius; smaller radii yield higher curvatures and vice versa. Ligands are spatially isolated at higher curvatures due to the steep surface gradient. As a nanosphere radius increases, the surface gradient decreases lipids and receptors have access to more surface area due to a smaller out-of-plane distance, which can be overcome by thermal fluctuations in the membrane.

Depending on the length of the ligand-receptor binding potential and with no imposed valency, more receptors could begin to interact attractively with the single ligand. Additionally, the ligand-receptor interaction energy (ϵ_{LR}), may be large enough that receptor heads begin to overcome the repulsive WCA potential used to maintain separation, causing them to cluster together.

To show that curvature can change the effective ligand valency, we simulated wrapping a range of spherical nanoparticles with radii of $7-12\sigma$. In each simulation performed here, 50% of the nanoparticle surface was covered with ligands, and ϵ_{LR} was scaled so that in a system where the valency, X, is 1 the maximum total energy contribution arising from ligand-receptor interactions, $E_{\mathrm{LR}}^{\mathrm{max}} = min(N_L, N_R)\epsilon_{LR}$, would be constant for all fully wrapped particles, regardless of their size. By scaling these interactions, we isolate the effect of nanoparticle curvature on valency. Caution was taken to ensure that the average distance between the

surface beads of the nanospheres remained constant as the radius increased.

Figure 2 shows the relationship between the valency and Gaussian curvature to be linear. The linearity is likely due to the circular area of the receptor patch, which grows as the nanoparticle curvature decreases, as both are functions of R^2. However, the relationship is slightly more complex as this pattern will only hold to a maximum valency, which may vary with simulation conditions, such as the cutoff of the ligand-receptor interaction strength. Additionally, if the radius were to continue to increase, there would likely be a limit that is reached due to spatial limitations preventing more receptors from binding.

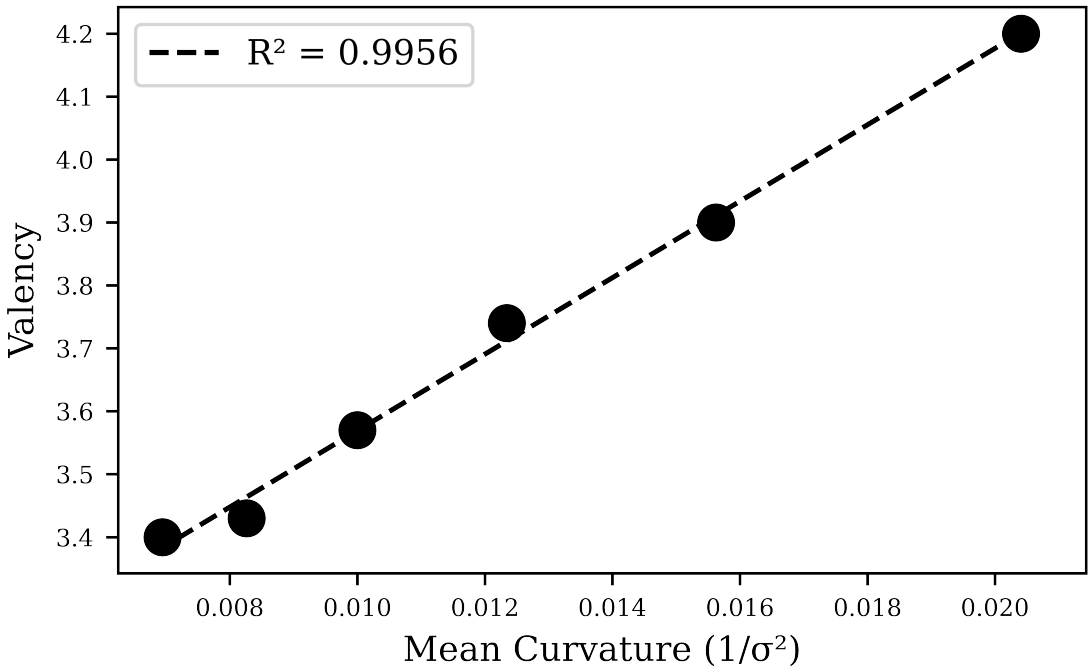

Figure 2: Relationship between the curvature of the nanospheres and the valency of their ligands. The dotted line is a linear regression of the data points, with the coefficient of determination, R^2, shown on the plot.

Next, the radius of the nanosphere is kept constant while the ligand density and ϵ_{LR} increase. Theoretically, as the two factors increase, the nanosphere should wrap faster as long as there are a sufficient number of receptors. Therefore, analysing the valency rather than the wrapping time is necessary to isolate any non-physical behaviours of the system. As shown

in Figure 3, the use of a pairwise potential purely dependent on distance leads to a change in the effective valency of ligands not only as a function of the nanosphere radius but also as a function of ligand coverage and the maximum ligand-receptor attraction ϵ_{LR}. Valency increases monotonically with ϵ_{LR} at low coverage because, as previously discussed, a stronger ligand-receptor attraction can compensate for the increased receptor-receptor repulsion due to a higher receptor concentration around a ligand. As more ligands are introduced, receptors pack uniformly onto the surface, converging towards a maximum valency of $X = 4.2$ for this system.

To correct the shortcomings of purely distance dependent potentials, we suggest using a different description to force a ligand's valency to a specific value, which should be determined based on the knowledge of the specific ligand-receptor pair to be simulated. To do this, we introduce a bond whenever a ligand and a receptor come within a certain distance and break if their distance exceeds a set limit, as described in the Methods. A bond can form if the number of bonds the ligand and receptor are already engaged in is below a given maximum value $X_{\max}$, thereby effectively imposing a specific valency. Formed bonds make particles interact with a bonding potential mimicking their distance-dependent interaction.

To properly characterize uptake speed in coarse grained systems, which can be highly dependent on receptor concentration and ϵ_{LR}, consistent comparative results are necessary. By this, we mean that two nanospheres' proportional uptake time, T_u, should remain consistent across similar models using distance-dependent ligand-receptor interactions. The uptake speed becomes meaningless if the proportional wrapping time between two spheres is measured without controlling valency.

Here we attempt two different approaches to modelling uptake, with and without imposing a maximum valence, with receptor concentrations of 20, 50, and 80%. Membranes with a lower concentration of receptors will reduce the likelihood of having multiple receptors per ligand, restricting the valency in scenarios that are not explicitly imposed. This restriction occurs because there will be fewer receptors available to bind to each ligand. In Figure 4,

Figure 3: Valency as a function of ligand coverage and ligand-receptor bond energy ϵ_{LR}, for a spherical nanoparticle of radius 7σ. Note the linear relationship between valency and ϵ_{LR}, with a decreasing slope as ligand coverage increases.

the percent error of the system with no imposed valence is shown, calculated using Equation 5

$$\%E = 100 * \frac{|T_u^{NV} - T_u^{V}|}{|T_u^{NV} + T_u^{IV}|/2} \tag{5}$$

where T_u^{NV} is the wrapping time of the system with no imposed valence, and T_u^{IV} is the wrapping time of the system with an imposed valence of $X = 1$.

A parabolic fit is applied to the data in Figure 4 with a coefficient of determination

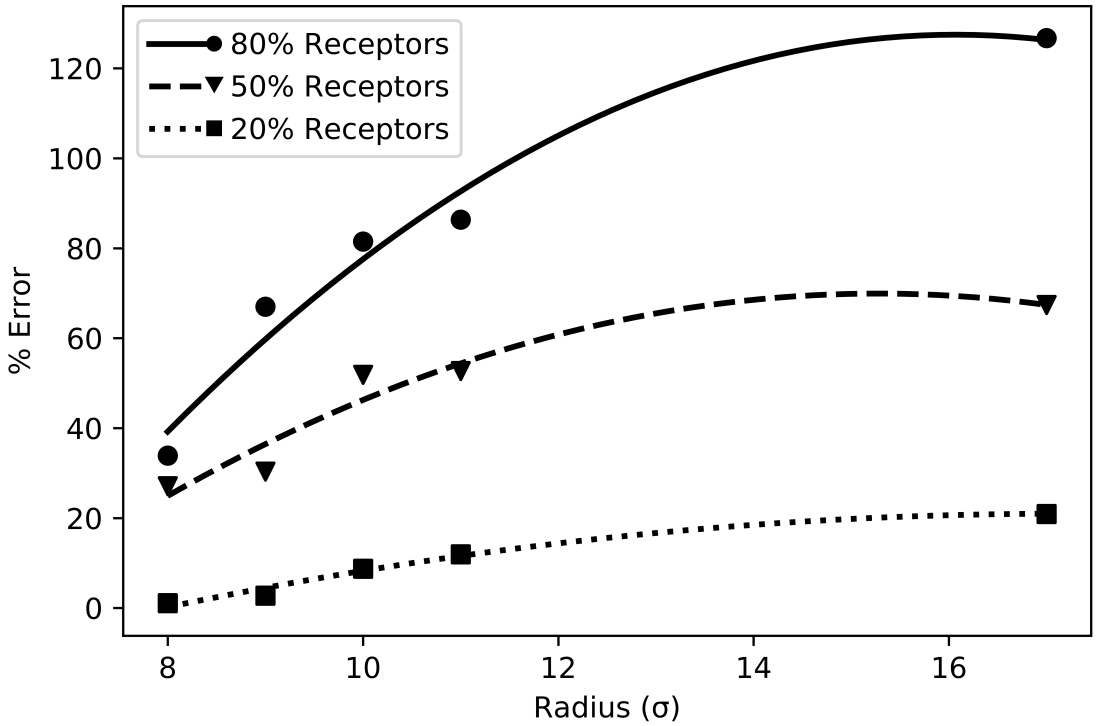

Figure 4: The comparative T_w of nanospheres with increasing radii. Both methods are fit with a parabolic dashed line, showing that the pairwise method fails to compare particles accurately.

above 0.95 for each receptor concentration. As the curvature of the nanosphere increases, with $1/R^2$, the valency increases, causing the nanospheres to wrap with increased speed, which likely approaches a limit when the maximum valency is reached. Therefore, the larger the nanosphere, the larger the valency, and the more erroneous the results. Most simulations in previous studies use a limited range of radii due to increased computational time, which may explain the difficulty in identifying the valency problem described here. Lower receptor concentrations reduce the valency when not imposed due to the lower probability of multiple receptors diffusing to the same ligand. The trade-off is that lower receptor concentrations result in longer simulation times, which is unnecessary for comparing nanoparticle T_u if the method described here is adopted.

One may think that a potential solution that could allow the use of these simple potentials

would be to rescale the effective value of the bond energy ϵ_{LR} to obtain any target valency. This solution would mean running simulations twice, once to determine $(\frac{1}{L}\sum_{n=1}^{L} U_{tail})$, and once after scaling ϵ_{LR}. Not only does this fail to rectify the original problem, but the research shown herein has exemplified the relationship between ϵ_{LR} and X, suggesting that this may not result in appropriate comparisons. Table 2 shows X for the nanospheres run in Figure 4, along with X after ϵ_{LR} has been rescaled using the following equation $\epsilon_{LR} = \epsilon_{LR_o}/X$, where ϵ_{LR_o} is the original ligand-receptor bond energy of $20k_BT\epsilon$.

Table 1: Calculated valency for nanospheres interacting with a membrane made of 50% receptors. No valency is imposed, and it is shown here that the valency is not easily controlled by scaling.

Radius (σ)	$\epsilon_{LR_o}(\epsilon)$	$X_{Original}$	$\epsilon_{LR}(\epsilon)$	X_{Scaled}
7	20	5.15	3.87	0.57
8	20	5.07	3.93	0.56
9	20	4.92	4.06	0.58
10	20	4.84	4.12	0.60
11	20	4.74	4.21	0.63
...	...	...	...	...
17	20	4.35	4.59	0.69

While the error is reduced due to the smaller increase in valency as the nanoparticle radius increases, there is no control over the ligand valency.

Conclusions

By modifying the curvature of the nanoparticle, the concentration of receptors, the density of ligands, or the strength and length of the potential between ligands and receptors, the valency of the system where none is imposed can change drastically. While the study was confined to spherical nanoparticles, other structures with non-continuous curvature can also be affected.

However, many of the details from previously published works are not necessarily invalidated by the artefacts presented here. Studies using lower receptor concentrations, smaller nanospheres, scaled ϵ_{LR}, and weaker ligand-receptor binding potentials are likely only mildly affected. But to ensure that methods are robust and repeatable, a proper consideration of valency must be taken. Therefore, the authors recommend that, given the inconsistencies demonstrated throughout this work, pairwise functions to model ligand-receptor interactions should be discontinued when possible, and valency be reported in the methods of each publication. All code necessary to recreate the results of this paper, and perform simulations in LAMMPS can be found at: https://github.com/shakespearemorton/Nano$_W rap$

References

(1) Villanueva-Flores, F.; Castro-Lugo, A.; Ramírez, O. T.; Palomares, L. A. Understanding cellular interactions with nanomaterials: Towards a rational design of medical nanodevices. **2020**, *31*.

(2) Stefan Willhelm,; Anthony J. Tavares,; Qin Dai,; Seiichi Ohta,; Julie Audet,; Harold F. Dvorak,; Warren C.W. Chan, Analysis of nanoparticle delivery to tumours. *Nature Reviews Materials* **2016**, *1*, 16014.

(3) Curk, T.; Dobnikar, J.; Frenkel, D. Optimal multivalent targeting of membranes with many distinct receptors. *Proceedings of the National Academy of Sciences of the United States of America* **2017**, *114*, 7210–7215.

(4) Morton, W.; Joyce, C.; Taylor, J.; Ryan, M.; Angioletti-Uberti, S.; Xie, F. Modeling Au Nanostar Geometry in Bulk Solutions. *Journal of Physical Chemistry C* **2023**, *127*, 1680–1686.

(5) Li, Y.; Kröger, M.; Liu, W. K. Shape effect in cellular uptake of PEGylated nanoparticles: Comparison between sphere, rod, cube and disk. *Nanoscale* **2015**, *7*, 16631–16646.

(6) Patel, S.; Kim, J.; Herrera, M.; Mukherjee, A.; Kabanov, A. V.; Sahay, G. Brief update on endocytosis of nanomedicines. *Advanced Drug Delivery Reviews* **2019**, *144*, 90–111.

(7) Cardellini, J.; Caselli, L.; Lavagna, E.; Salassi, S.; Amenitsch, H.; Calamai, M.; Montis, C.; Rossi, G.; Berti, D. Membrane Phase Drives the Assembly of Gold Nanoparticles on Biomimetic Lipid Bilayers. *Journal of Physical Chemistry C* **2022**, *126*, 4483–4494.

(8) Lee, Y. K.; Lee, H.; Nam, J. M. Lipid-nanostructure hybrids and their applications in nanobiotechnology. *NPG Asia Materials* **2013**, *5*, 1–13.

(9) Koch, A. H.; Morsbach, S.; Bereau, T.; Lévêque, G.; Butt, H. J.; Deserno, M.; Landfester, K.; Fytas, G. Probing Nanoparticle/Membrane Interactions by Combining Am-

phiphilic Diblock Copolymer Assembly and Plasmonics. *Journal of Physical Chemistry B* **2020**, *124*, 742–750.

(10) Rennick, J. J.; Johnston, A. P.; Parton, R. G. Key principles and methods for studying the endocytosis of biological and nanoparticle therapeutics. *Nature Nanotechnology* **2021**, *16*, 266–276.

(11) Rees, P.; Wills, J. W.; Brown, M. R.; Barnes, C. M.; Summers, H. D. The origin of heterogeneous nanoparticle uptake by cells. *Nature Communications* **2019**, *10*.

(12) Xie, X.; Liao, J.; Shao, X.; Li, Q.; Lin, Y. The Effect of shape on Cellular Uptake of Gold Nanoparticles in the forms of Stars, Rods, and Triangles. *Scientific Reports* **2017**, *7*.

(13) Yi, X.; Gao, H. Kinetics of receptor-mediated endocytosis of elastic nanoparticles. *Nanoscale* **2017**, *9*, 454–463.

(14) Zhang, X.; Ma, G.; Wei, W. Simulation of nanoparticles interacting with a cell membrane: probing the structural basis and potential biomedical application. *NPG Asia Materials* **2021**, *13*, 52.

(15) Vácha, R.; Martinez-Veracoechea, F. J.; Frenkel, D. Receptor-mediated endocytosis of nanoparticles of various shapes. *Nano Letters* **2011**, *11*, 5391–5395.

(16) ming Ding, H.; qiang Ma, Y. Role of physicochemical properties of coating ligands in receptor-mediated endocytosis of nanoparticles. *Biomaterials* **2012**, *33*, 5798–5802.

(17) Yang, K.; Ma, Y. Q. Computer simulation of the translocation of nanoparticles with different shapes across a lipid bilayer. *Nature Nanotechnology* **2010**, *5*, 579–583.

(18) Li, Z.; Wang, J.; Wei, Q.; Qi, Z.; Zhou, L.; Li, J. In silico insights into the receptor-mediated endocytosis of virus-like nanoparticles. *Chemical Physics Letters* **2022**, *790*.

(19) Varilly, P.; Angioletti-Uberti, S.; Mognetti, B. M.; Frenkel, D. A general theory of DNA-mediated and other valence-limited colloidal interactions. *Journal of Chemical Physics* **2012**, *137*.

(20) Shen, Z.; Ye, H.; Li, Y. Understanding receptor-mediated endocytosis of elastic nanoparticles through coarse grained molecular dynamic simulation. *Physical Chemistry Chemical Physics* **2018**, *20*, 16372–16385.

(21) Li, Y.; Yue, T.; Yang, K.; Zhang, X. Molecular modeling of the relationship between nanoparticle shape anisotropy and endocytosis kinetics. *Biomaterials* **2012**, *33*, 4965–4973.

(22) Huang, C.; Zhang, Y.; Yuan, H.; Gao, H.; Zhang, S. Role of nanoparticle geometry in endocytosis: Laying down to stand up. *Nano Letters* **2013**, *13*, 4546–4550.

(23) Thompson, A. P.; Aktulga, H. M.; Berger, R.; Bolintineanu, D. S.; Brown, W. M.; Crozier, P. S.; in 't Veld, P. J.; Kohlmeyer, A.; Moore, S. G.; Nguyen, T. D.; Shan, R.; Stevens, M. J.; Tranchida, J.; Trott, C.; Plimpton, S. J. LAMMPS - a flexible simulation tool for particle-based materials modeling at the atomic, meso, and continuum scales. *Computer Physics Communications* **2022**, *271*, 108171.

(24) Weik, F.; Weeber, R.; Szuttor, K.; Breitsprecher, K.; de Graaf, J.; Kuron, M.; Landsgesell, J.; Menke, H.; Sean, D.; Holm, C. ESPResSo 4.0 –an extensible software package for simulating soft matter systems. *The European Physical Journal Special Topics* **2019**, *227*, 1789–1816.

(25) Dasgupta, S.; Auth, T.; Gompper, G. Shape and orientation matter for the cellular uptake of nonspherical particles. *Nano Letters* **2014**, *14*, 687–693.

(26) Cooke, I. R.; Kremer, K.; Deserno, M. Tunable generic model for fluid bilayer membranes. *Physical Review E - Statistical, Nonlinear, and Soft Matter Physics* **2005**, *72*.

(27) Cooke, I. R.; Deserno, M. Solvent-free model for self-assembling fluid bilayer membranes: Stabilization of the fluid phase based on broad attractive tail potentials. *Journal of Chemical Physics* **2005**, *123*.

(28) Fowler, P. W.; Hélie, J.; Duncan, A.; Chavent, M.; Koldsø, H.; Sansom, M. S. Membrane stiffness is modified by integral membrane proteins. *Soft Matter* **2016**, *12*, 7792–7803.

(29) Smith, D. J.; Klauda, J. B.; Sodt, A. J. Simulation Best Practices for Lipid Membranes. *Living Journal of Computational Molecular Science* **2019**, *1*.

(30) Banerjee, A.; Berezhkovskii, A.; Nossal, R. Kinetics of cellular uptake of viruses and nanoparticles via clathrin-mediated endocytosis. *Physical Biology* **2016**, *13*.